

Constant Power Factor Mode of Grid- Connected Photovoltaic Inverter for Harmonics Distortion Assessment

Muammar Zainuddin*[‡], Frengki Eka Putra Surusa*, Syafaruddin**, Salama Manjang**

*Department of Electrical Engineering, Faculty of Engineering, Universitas Ichsan Gorontalo, 96138 Gorontalo City-Indonesia

** Department of Electrical Engineering, Faculty of Engineering, Universitas Hasanuddin, 92119 Gowa-Indonesia

(muammarz@unisan.ac.id, frengki@unisan.ac.id, syafaruddin@unhas.ac.id, salamamanjang@unhas.ac.id)

[‡] Corresponding Author; Muammar Zainuddin, 96138, Tel: +62 852 5866 7668, muammarz@unisan.ac.id

Received: 20.07.2020 Accepted:23.08.2020

Abstract- The increased active power injection of the grid-connected Photovoltaic (PV) inverters has led to some challenges in the power quality issues. The PV inverters have been recommended in the technical standard requirements in order to control the reactive power supply into the grid. The purpose of this study is to investigate the correlation of the power factors to total harmonics distortion (THD) in a 30 kWp grid-connected PV inverter using two different operating modes. This research presents analyses of the statistical results of power quality parameters such as the changes in relative and reactive power, THD on current and voltage, and harmonic components of current and inverter voltage at different loads. The power quality parameters is assessed by using the Var regulation based on a constant power factor (CPF) and compared with the Var regulation based on changes in grid voltage (Q(U)). The unity and non-unity PF is simulated with high and low capacitive level. The results showed that THDi and THDv were less than 5% when the inverter approached nominal power. The non-unity PF constant inverter produces lower harmonic distortion than the unity PF. The simulation results found that the harmonic component of the current increased by more than 7% in the 7th order when the active power was less than 9% of the nominal power. However, reactive power regulation is proportionally constrained to prevent overvoltage of the inverter. The presented results are useful in fulfilling the technical requirements associated with the operating mode of the grid-connected PV inverters.

Keywords- Power Quality; Photovoltaic Grid-Connected; Reactive Power; Constant Power Factor; Harmonics Analysis.

1. Introduction

The application of grid-connected photovoltaic (PV) solar plants is increasingly popular in various tropical countries. Grid-connected PV is a solar power generation model that is easily implemented to maximize the energy potential of an area. It is categorized as Distributed Energy Resources (DER) that is environmentally friendly, available throughout the year and has an easily-implemented technology. The association electric power system can build PV plants and export their power into the grid utility. Some countries have made technical standard rules on its integration in distribution and transmission lines. The harmonic control requirements of grid-connected PV in power systems have been recommended in technical

standards [1]. The operational challenges of PV plants integrated with the grid need to consider the power continuity, quality and its impact on the grid [2]–[4]. The intermittent characteristics of a PV plant has the ability to affect all power quality variables in an electrical power system [5]–[9].

The increase in penetration of PV inverters brings with it problems of reactive power and voltage in the distribution network. The increase in reactive power requirements has affected power quality in PV generation and the consumer side [10]. All AC loads contain inductance or capacitance therefore they require active and reactive power to operate. In the past, all grid-connected PV inverters operated in a unity power factor mode and supplied active power

requirements. In the practice of buying and selling electricity by utilities, payment is made on only transfers of active power. The PV inverters that produce reactive power can reduce active power production [11]. These conditions cause losses for the PV plant association because it reduces their income. However, reactive power compensation from the PV plant has a positive impact on improving its quality, reducing losses, and improving the voltage profile on the grid [11]–[14]. In some countries, the utility has changed the interconnection an interoperability standard for grid-connected PV plants with distributed energy resources (DER) used to apply reactive power regulation and voltage control [15].

The latest smart inverter technology currently play the role of injecting active and reactive power through a control or power management strategy [16], [17]. The reactive power compensation of the PV system needs to be in the proportional range required by the grid load without having an effect on the increase in the voltage outside the operating standard [10], [11], [16]. PV inverters can be set to supply a certain ratio between active and reactive power, or dynamically adjusted on a grid that changes periodically. Reactive power regulation on the inverter is related to its power factor level. According to Mack Grady [18], the value of the power factor is related to the power quality and use in limiting harmonic distortion. Harmonic distortion in grid-connected PV systems is caused by non-linear loads [19]–[21], frequency switching variables in inverters [22], [23], and fluctuations in solar radiation [6], [24], [25]. The characteristics of current harmonic emissions in PV inverters under different voltage supplies have been evaluated by Xiao Xu et al. [26]. Similarly, Christine et al. [27] stated that the characteristics of harmonic distortion in distribution feeders were due to the inclusion of PV distributed generation (PVDG). Harmonics injected by PVDG are partly additive and contribute to an increase in total harmonic distortion in the distribution feeder. An increase in voltage THD occurs at the PV solar farm terminals connected to the distribution network during cloudy weather [28].

Nowadays, grid-connected PV plants are needed to operate and implement reactive power regulations under the fluctuating voltage and intensity of solar radiation. Several methods have been used to determine the reactive power regulation on inverters to limit harmonic distortion and improve power quality. Hassaine et al. [29] proposed a digital power factor and reactive power regulation using a field-programmable gate array (FPGA). The results of Hassaine's study experimentally showed the feasibility of power factor control and its reactive injection to reduce the THD of the inverter into the grid. Sigifredo Gonzalez et al. [30] described the effect of non-unity power factor on PV inverters to support grid functions. Renukadevi and Jayanand [31] described reactive power compensation to reduce the harmonics of current in a grid-connected PV inverter when its power factor approaches one. The power factor control on the PV inverter is intended to increase the voltage profile of the distribution feeder [32]. Therefore, reactive power regulation through adequate power factor management is needed to assess the effect on the power quality of the grid-connected PV.

This research was carried out on a 30 kWp inverter used in grid-connected PV plants in Gorontalo-Indonesia. The inverter operates in Q(U) mode, with the ability to transfer reactive power based on changes in grid voltage with the production of harmonics above 3%. This study investigated the relationship between power factor towards total harmonics distortion on current and voltage in the inverter in two different operating modes. Furthermore, THD assessments were carried out via experimental measurements on a Q(U) mode inverter and compared to a simulated constant power factor (CPF) mode inverter. The CPF method is used to determine the maximum reactive power regulation that needs to be transferred into the grid. The simulation of the CPF inverter utilized the constant non-unity PF method with high and low level (capacitive) variations and compared with the constant PF unity method. The first assessment discussed the ability of the inverter reactive power as a function of the relative power and RMS voltage change. Meanwhile, the second assessment analyzed the relationship between THDi and THDv as a function of the inverter's relative power. The third assessment discussed the relationship of THDi and THDv as a function of reactive power. Meanwhile, the fourth assessment analyzes changes in the value of the harmonic components of the current and voltage of the inverter under different loading conditions. This paper is useful to fulfill the technical requirements of the grid-connected PV operators by considering the operating mode of an inverter.

2. Materials and Methods

2.1. Grid-Connected Photovoltaic System

The inverters type SG30xxx with a size of 30 kWp was used by the grid-connected PV plant in Gorontalo-Indonesia. Figure 1 shows the string topology of grid-connected PV inverter connected to the distribution line. Each inverter unit uses an MPPT to maximize the conversion of DC to AC power, while the PV station subsystem uses a step-up transformer clutch to raise the voltage level to the distribution system. The inverter input power is sourced from a 240 Wp PV array connected in series and parallel. The power flow analysis of the grid-connected photovoltaic system is the foundation of studying steady-state characteristics of large-scale solar PV integrating into the power grid [33].

The initial principle of operation on a grid-connected PV inverter is used by the inverter to detect the voltage and current on the grid. The automatic synchronization of the inverter with the grid is by obtaining the same signal amplitude, frequency and phase angle. The inverter operates at the level of the upper and lower limits of the specified voltage. It is also equipped with an overcurrent protection to prevent the AC output current from exceeding the rating of minimum short-circuit and maximum load current. The frequency at the inverter does not need to exceed the allowable upper limit, with the anti-islanding protection system used to protect the inverter working without grid load.

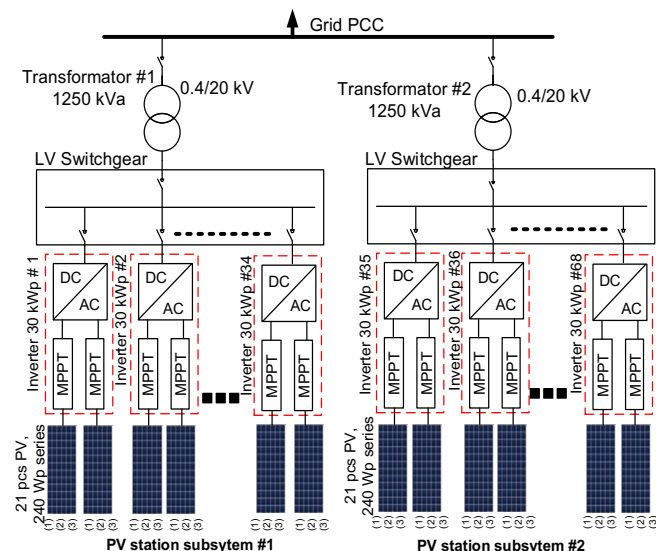


Figure 1. The topology of grid-connected PV system in Gorontalo-Indonesia.

2.2. Power Quality Profile

Figure 2 shows the relationship between the intensity of solar radiation with the three-phase RMS voltage on inverter number 1 for one measurement day on April 4, 2019. The measuring instrument of voltage and current harmonic distortions is Hioki 3286-20. Changes in the intensity of solar radiation affect the production of active power and voltage of the inverter with the highest peak of solar radiation of 1011 W/m^2 obtained at 10:20:00 AM. Figure 3 shows the inverter output power profile during the measurement periods, which are active, reactive, apparent power, and power factor. The AC nominal power of the inverter (P_{nom}) is 30.00 kW, or the maximum power rating (S_n) of the inverter output is 33.120 kVA, and during the measurement period, the highest active power (P_{ac}) obtained is 28.42 kW. Figure 4 shows the total harmonic distortions of voltage and current at the PV inverter output measured for a day with data obtained when the inverter operates in Q(U) mode.

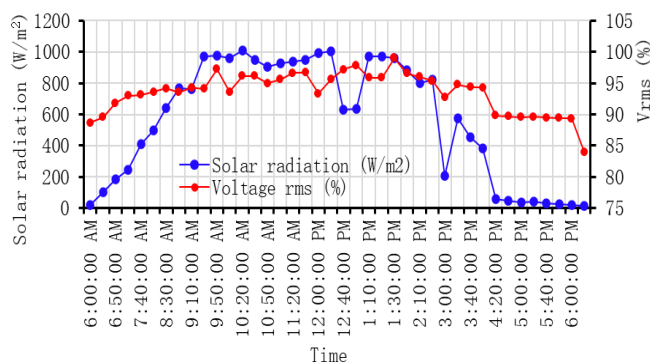


Figure 2. Solar radiation intensity and RMS voltage

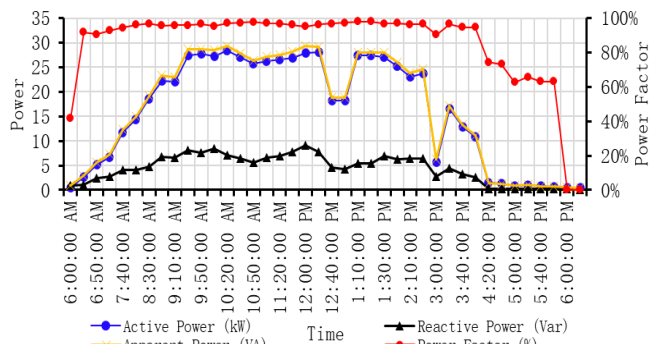


Figure 3. Active, reactive, apparent power and power factor

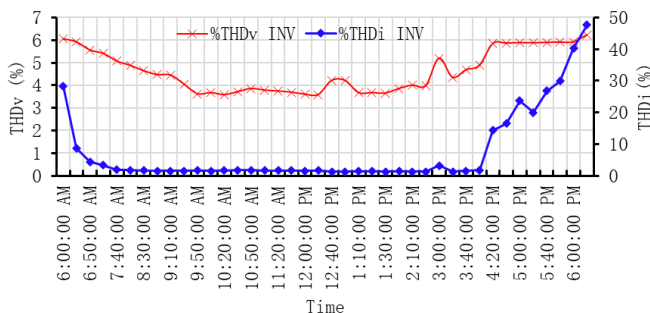


Figure 4. Measurement of THDi and THDv

2.3. Power Factor Management Strategy

The interconnection standard of distributed energy resources (DER), the reactive power regulation generally uses four different operating modes. Constant power factor (CPF) mode is a regulation based on PF (Unity and Non-unity power factor) parameters, Constant reactive power mode (Var fixed), mode Q(P) is a regulation based on active-reactive power, and mode Q(U) are regulation based on changes in inverter reactive power output and grid voltage. In this study, the experimental measurements of inverters operate in Q(U) mode and are compared with simulations of the CPF.

The 30 kWp inverter measured in Q(U) mode has the ability to produce or absorb reactive power. In this mode, the inverter controls its reactive power output in accordance with a linear characteristic of the grid voltage. The inverter simulation in CPF mode is used to control the reactive power output according to the operating power factor. When this CPF mode is activated, the inverter exports maximum reactive power according to the PF target. Hua Li et al. [13] and Saša Vlahinić et al. [14] stated that the impact of reactive power compensation on the RMS voltage quality of the inverter affects the voltage of the harmonic component. The CPF operating mode is used to calculate the harmonic contribution, which is affected by changes in reactive power.

The power capacity (VA) of the inverter is determined through cos/sine rules with apparent power used to describe the amount of electricity usable by the equipment. The inverter capacity consists of active power (W_{ac}) and reactive power (Var) with relative power to is the ratio between active and nominal power (P_{ac}/P_{nom}). The mode Q(U) inverter measurement is carried out by setting the upper and lower

limit constraints of the inverter voltage. This mode creates an inconsistent of fluctuating effect on the PF value and reactive power. Meanwhile, the simulation carried out on the CPF mode inverter is used to determine the value of the constant power factor proportionately and the maximum reactive power. Figure 5 shows the reactive power regulation that is achieved as a function of the nominal power of the inverter. In CPF mode, the converted active power of the inverter affected the reactive power output and used to maintain a constant ratio between the levels of active and apparent power. The total VA output is not allowed to exceed the maximum value of the inverter size due to its ability to decrease the active power output to be less than 100% when the constant power factor specified is below this percentage. Figure 5 (a) shows the nominal power and reactive power limits for each PF setting constant. The PF problem is overcome by operating the inverter according to the grid load characteristics, with its loads limited by maximum current and reactive power limits. Figure 5 (b) shows the reactive power capability with inverter size on the standard voltage limit of the inverter. The simulated 30 kWp has the ability to provide a certain percentage from the ratio of reactive and apparent power. Its adjustment occurs within the standard operating voltage limits.

Equation (1) shows the conventional calculation of the power factor obtained between the active ratio and apparent power. The power factor determines the amount of active power transferred to the grid and determines the value of injection or absorbs reactive power. Inverters operating at CPF mode need to apply regulations by setting a limit of maximum reactive power (Q_{max}).

$$\cos \theta = \frac{P}{S} = \frac{\text{Watt}}{V_{rms} \cdot I_{rms}} \quad (1)$$

In the triangle rule of the power system, apparent power (S_{inv}) is obtained by adding up the active power (P_{inv}) and reactive power (Q_{inv}). In this study, the active power of the inverter depends on the conversion of PV array power. S_{max} is the maximum power capacity rating on a PV inverter. Therefore, the calculation of active power (P_{ac}) and maximum reactive power (Q_{max}) of the inverter transferred to the grid is expressed in equations (2) and (3).

$$P_{ac} = S_{inv} * \cos \theta \quad (2)$$

$$Q_{max} = |Q_{inv}| < \sqrt{(S_{max})^2 - (P_{ac})^2} \quad (3)$$

The main purpose of operating a PV inverter in Q(U) and CPF mode is to produce an inverter reactive power limit. The inverter requires constraints that are set at the voltage V_{L1} and V_{L2} which are the lower V limit that can be set in the range of 90%...80%. V_{U1} and V_{U2} are upper V limits that can be set in the range of 100%...105%. Reactive power output based on a constant PF can be obtained according to Eq. (4)–Eq. (6).

$$V_{grid} < V_{L2} = Q_{max} \text{ (upper PF capacitive) and}$$

$$V_{U2} < V_{grid} = -Q_{max} \text{ (lower PF inductive)} \quad (4)$$

$$V_{L2} < V_{grid} < V_{L1} = \frac{V_{L1}-V_{grid}}{V_{L1}-V_{L2}} \times Q_{max} \quad (5)$$

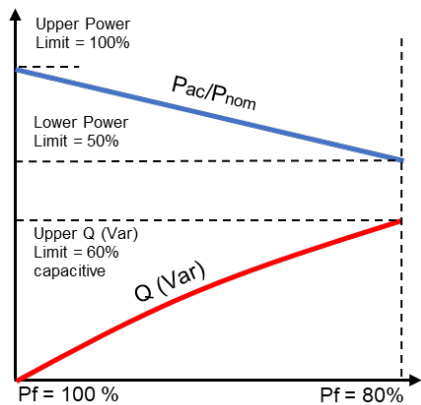
$$V_{U1} < V_{grid} < V_{U2} = -\left(\frac{V_{U1}-V_{grid}}{V_{U1}-V_{U2}}\right) \times Q_{max} \quad (6)$$

2.4. Total Harmonics Distortion Analysis of PV Inverters Grid-connected

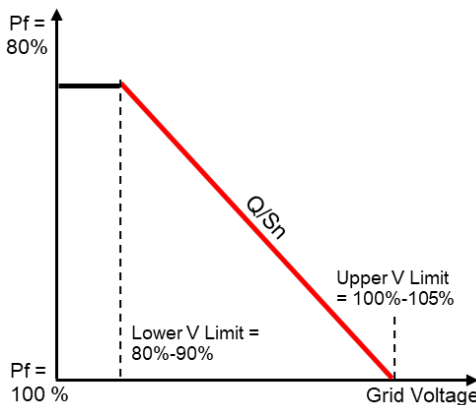
The percentage limit for total harmonic current and voltage distortion is recommended in Std. IEEE 519-2014. Total voltage harmonic distortion (THDv) is the ratio of the RMS (Root Mean Square) value of the harmonic component (U_n) to the RMS voltage (U_1). Total current harmonic distortion (THDi) is the ratio between the RMS current values of the harmonic (I_n) with the fundamental component (I_1) expressed in percent (%). The sequence of the harmonic component order is expressed in symbol H. The THD of perfect sine wave is zero percent, while the mathematical formula in Eq. (7) and Eq. (8) for the THDv and THDi of nonsinusoidal waves [13] [34].

$$THD_i = \sqrt{\sum_{n=2}^H \left(\frac{I_n}{I_1}\right)^2} \times 100\% \quad (7)$$

$$THD_v = \sqrt{\sum_{n=2}^H \left(\frac{U_n}{U_1}\right)^2} \times 100\% \quad (8)$$



(a) Power factor as a function of reactive power.



(b) Reactive power capability to grid voltage.

Figure 5. Reactive power capability curve on CPF mode inverter

2.5. Data Collection and Limitation

This research presents measurements data records of inverter that operate in Q(U) mode. Data was collected at the grid-connected PV generator for three days (03, 04, 05 April 2019). However, only data from April 4, 2019 were selected for use in this study with justification describing the low, medium and high solar radiation intensity. Data records were obtained through the control logger unit installed in the PV plant area. Measurement data samples in the control logger unit are set at 40 time-settings (6:00:00 AM - 6:00:00 PM) and the variables obtained were solar radiation intensity, ambient temperature, PV panel temperature, inverter RMS voltage, inverter RMS current, active power, reactive power, apparent power, and inverter power factor. All data records were validated by the operator to avoid errors with the power load received by the inverter from the distribution grid. THDi/THDv and harmonic components of current/voltage in the inverter were measured using Hioki 3286-20 and validated to determine the precision. The measuring instrument can assess the current and voltage harmonic components up to the 20th order and limits the assessment of those above 20. The time settings for measuring current and voltage harmonic distortion variables in the inverter are adjusted to the setting time on the control logger unit. This is applied in order for the harmonic distortion sample is matched with the data logger.

Grid-connected PV inverters with CPF mode are modeled and simulated using the software. The simulated inverter parameters are adjusted to the measurement data obtained through the control logger unit. In accordance with the agreement with the PV operator, this paper does not present the PV array and inverter brands; rather it is in the device datasheet. The simulated input parameters described the same conditions in the PV system with the accuracy results and used to avoid an error. The value of THDi/THDv and current/voltage harmonics component of each order is obtained through software calculation results. All simulation data have been validated to avoid calculation errors on the software.

3. Results and Discussion

3.1. Inverter Constant Power Factor Mode

This section presents a discussion on the comparison of the experimental measurement results inverter mode Q(U) with the simulation results of PV inverters in the non-unity and unity PF. The Q(U) mode inverter is used to compensate for the reactive power due to changes in grid voltage. These conditions describe the corrected power factor for each change in grid voltage. This is different from the results of simulations when the inverter operates in CPF mode. When CPF mode is simulated, the inverter operates at the specified power factor limit. Figure 6 shows the comparison of the reactive power output as a function of the inverter relative power in two different operating modes. Different levels of constant PF produce a constant ratio between relative and reactive power. When the active power output of the inverter changes based on the intensity of the solar radiation received by the PV array, the inverter varies the reactive power production according to the power factor target. In the simulation, the low and high nominal power categories are determined in the range of 0%...50% and 50%...100%. This shows that the inverter with the unity power factor model does not compensate for reactive power.

Figure 7 shows the comparison of the reactive power capability as a function of the inverter's voltage. A constant power factor value that decreases by 2% under 100% can increase the ratio of reactive power supply to apparent by 17% (PF 98%). Inverters that operate at a power factor below 90% (lower PF) and the ratio of maximum reactive power to maximum apparent power decreases can cause the inverter operating voltage to rise by more than 100% (Upper V limit). According to Kaveh Rahimi et al. [16], PV inverters with fixed power factor control cause voltage deviations when the inverter injects or absorbs reactive power. However, these conditions can be anticipated by establishing a constant power factor that is proportional to the characteristics of the grid load. The inverter voltage is in the range of 80%...90% and 100%...105% for the lower and upper V limit.

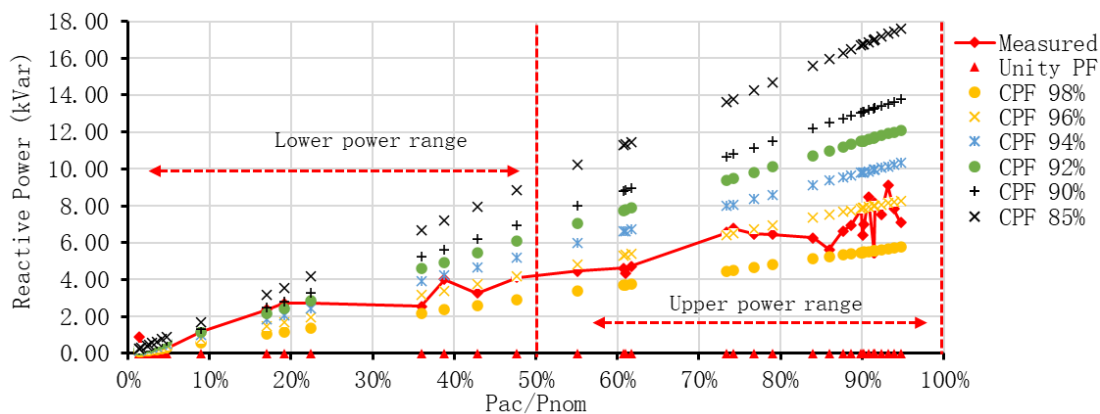


Figure 6. Reactive power output as a function of relative power

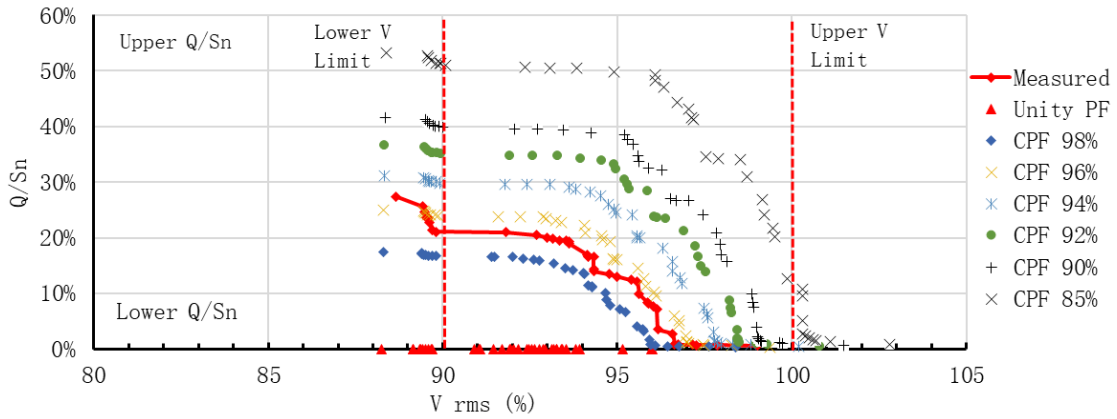


Figure 7. Reactive power capability as a function of Vrms.

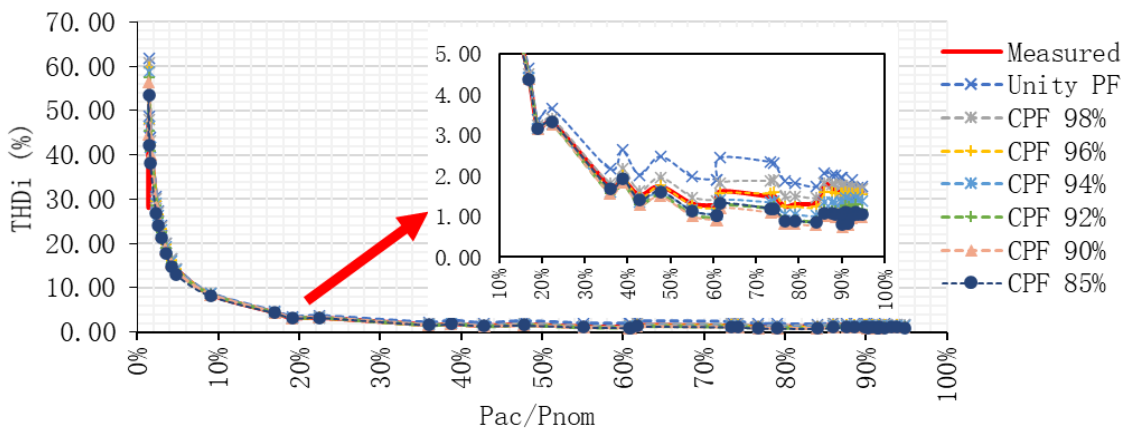


Figure 8. THDi as a function of relative power

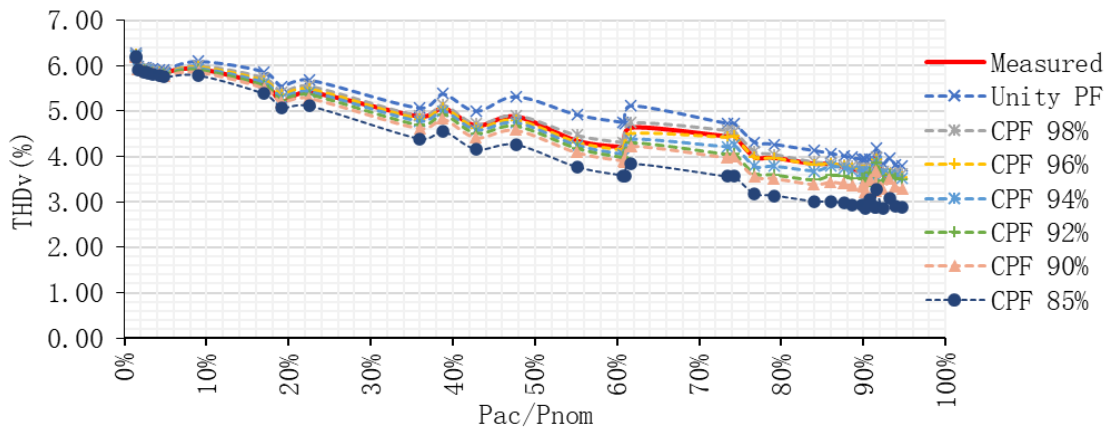


Figure 9. THDv as a function of relative power

3.2. Total Harmonics Distortion Assessment with Relative Power

Relative power describes the ratio of the active power of the inverter which depends on solar radiation to the nominal power of the inverter. Figure 8 shows the relationship of THDi to the inverter relative power from the measurement and simulation results in different operating modes. In Fig. 8 can be observed that the comparison of the experimental

measurements and simulation showed that the relative power of inverters less than 10% led to an increase in THDi values by more than 5%. The inverter show the change in the corrected power factor is based on the output, and these conditions contribute to the fluctuating of the THDi. The values tend to increase in a long duration with more frequencies. For inverters that only inject active power into the network, the current supplied needs to be in the same phase with similar voltage waves [35].

Table 1 shows the statistical analysis of THDi based on changes in the relative power of the inverter and compared with other studies. A higher THDi value is observed when the inverter operates in unity PF mode. The inverter manufacturers have a claim that their inverters provide a THD < 3% at nominal power. Figure 9 shows the relationship between the total harmonic distortion of voltage and the relative power of the inverter. The results of experimental measurements show that a THDv is less than 5% when the relative power is greater than 35%. The simulation results show that a THD is less than 5% when

the inverter's relative power output is above 30%. However, when the inverter operates in unity PF mode, it produces a higher THDv compared to the non-unity PF. This condition shows that the level of power factor has an impact on changes in THDv. A small inverter produces a relatively large THDi when a power level is below its nominal, however, the THDv is in an acceptable range according to technical standards [35]. Therefore, the power factor needs to be determined in relation to the inverter size to limit harmonic distortion.

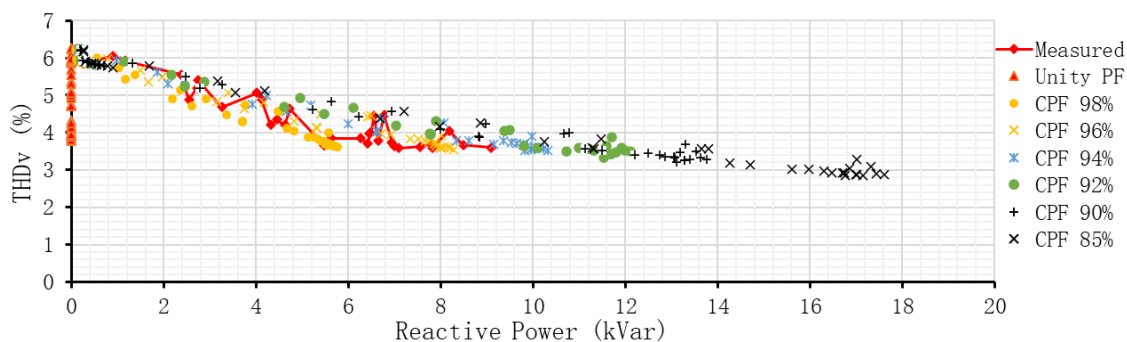
Table 1. Comparison of THDi based on the relative power of inverters

Compared Results	PF	Relative Power						
		5%	10%	20%	30%	50%	75%	
Rampinelli [34]	THDi at 0.95 PF	49.986	31.22	15.904	9.406	5.864	4.168	
	THDi at Unity PF	61.854	30.958	16.272	9.811	6.447	4.078	
A. Elkholy [36]	THDi at 0.95 PF	82.253	34.173	15.427	6.664	5.963	4.139	
	THDi at Unity PF	75.943	32.496	15.668	9.262	6.211	4.185	
		Relative Power						
	PF	4.80%	9.00%	19.13%	35.97%	74.23%	79.07%	90.03%
CPF Proposed	THDi at 0.96 PF	14.15	8.72	3.19	1.68	1.61	1.25	1.58
	THDi at 0.94 PF	13.95	8.63	3.16	1.60	1.38	1.06	1.34
	THDi at 0.92 PF	14.36	8.79	3.39	2.16	2.32	1.82	1.95
	THDi at Unity PF	14.36	8.79	3.39	2.16	2.32	1.82	1.95

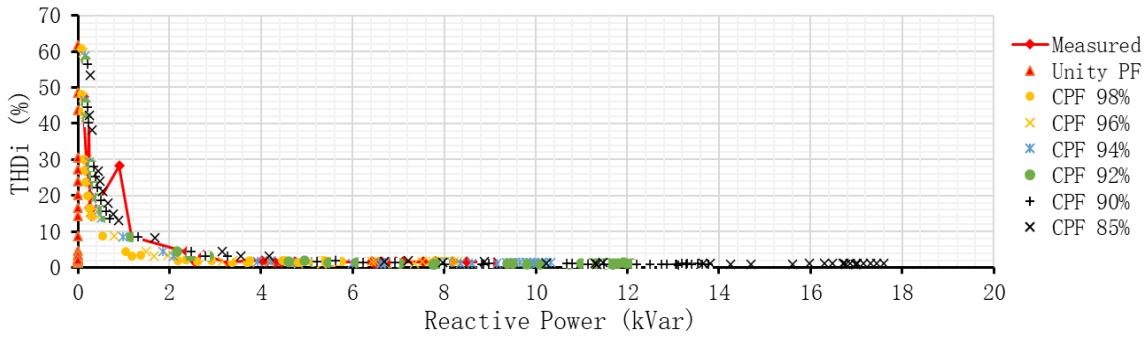
3.3. Total Harmonics Distortion Assessment with Reactive Power

This section discusses the impact of reactive power regulation through the CPF method on THDi and THDv in the inverter. The reactive power output transferred to the grid depends on the active power output of the inverter. In the simulation, the maximum reactive power limits are determined by a constant power factor. A constant ratio is obtained between the active and reactive power transferred to the grid. An increase in the reactive power output of inverter

leads to the total harmonic distortion of current and voltage less than 5%. Therefore, the operation of the inverter is in the upper power range. Figure 10 (a) and (b) shows the relationship of THDi and THDv with reactive power based on different operating modes. Simulation results show that the THDi is less than 5% when reactive power produce is more than 1 kVar for all levels of constant PF besides unity PF. THDv decreases along with an increase in the inverter's reactive power production. The inverter technology needs to limit harmonic distortion when the reactive power production is low.



(a) THDi as a function of reactive power



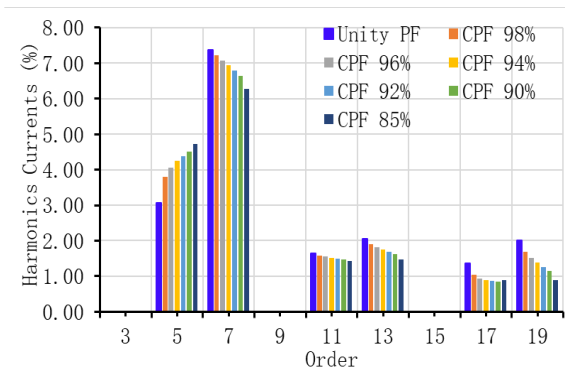
(b) THDv as a function of reactive power

Figure 10. Relationship of THDi and THDv to the reactive power

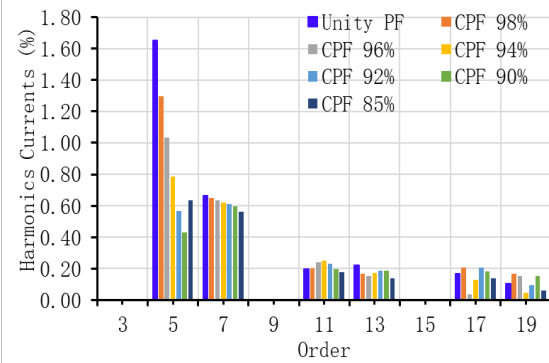
3.4. Analysis of Harmonic Currents and Harmonic Voltages

This section discusses the simulation results of the current and voltage harmonic components in the odd order. The currents and voltages harmonics components analyzed and compared at 9% and 79% of nominal power for different constant PF levels. According to Std. IEEE 519-2014, the harmonic limit of current for a system rating of 120 V to 69 kV of order $3 \leq h < 11$ at the ratio of the maximum short circuit with a maximum load of $20 < 50$ is below 7%. Figure 11 (a) and (b) shows harmonic components of the current when the inverter power output is 9% and 79% of nominal power. Harmonic currents increase above 7% in the 7th order (PF 100%; 98% and 96%). When the inverter’s power increases, the constant power factor limits the harmonic components of 7th to 19th orders by less than 1.00%.

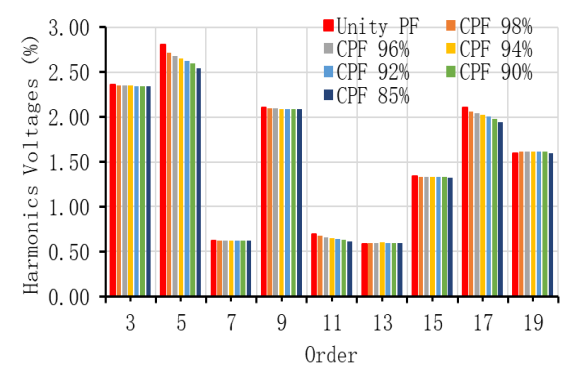
However, it should be noted that the 5th order harmonic currents becomes higher when the unity power factor mode is activated. The first odd-order harmonics are responsible for the level of distortion in the inverter [34]. According to A. Elkholly [36], harmonic currents increase due to a rise in voltages and the harmonic contribution in low, medium or high power varies according to the inverter model and network conditions. The harmonic voltages at 9% and 79% of nominal power as shown in Fig. 11 (c) and Fig. 11 (d). The harmonic voltages are distributed in all odd orders. The simulation results show that the first voltage harmonic occurs in 3rd order. The analysis results showed the correlation of the power factor with the contribution of each voltage harmonic. The percentage of voltage harmonic components is still in the limits of the specified technical standards.



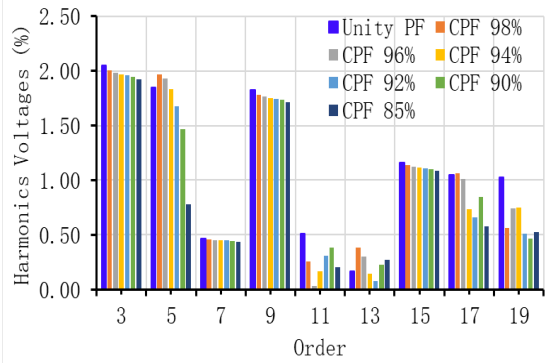
(a) Harmonics currents at 9% of P_{nom}



(b) Harmonics currents at 79% of P_{nom}



(c) Harmonics voltages at 9% of P_{nom}



(d) Harmonics voltages at 79% of P_{nom}

Figure 11. Current and voltage harmonics of the inverter CPF mode

4. Conclusion

This paper presents the assessment results for the performance of a 30 kWp inverter used in solar power plants connected to a distribution network. The characteristics of the inverter in different operating modes were compared by carrying out experimental measurement and simulation. The constant power factor method is proposed and simulated to illustrate the reactive power regulation of the inverter. Various levels of constant power factor capacitive are simulated from the values of 98%, 96%, 94%, 92%, 90% and 85%, which describe the upper and lower PF. The inverters with unity PF mode (100%) are simulated with the results are compared. The constant power factor illustrates the capability of the inverter to maintain a constant ratio between active and reactive power. The results of the statistical analysis assess the correlation between the level of power factor with the total harmonic distortion of current and voltage in the inverter. Furthermore, an increase in the ratio of active power output to the nominal power of the inverter tends to limit the occurrence of harmonic distortion. THDi increase when the relative power of the inverter is less than 10% and decreases by less than 5% when it approaches nominal power. Inverters that operate in unity PF mode produce higher THDv compared to non-unity CPF. This condition describes that the level of power factor affects different THDv. However, inverters with too lower power factor lead to overvoltages outside the operating limits. The simulation results of CPF showed that the components of the current and voltage harmonics in the inverter were obtained higher in low order. When the inverter's power output approaches nominal the harmonic content decreases. The analysis results presented are considered by PV plant operators to maximize system performance and support grid power quality. The determination of the CPF needs to be proportional to the possibility of anticipating the presence of negative effects. Continuation in this study investigates changes in power factor on the grid due to the reactive power injection of PV inverters and their impact on the harmonic distortion in the distribution network.

Acknowledgements

The Authors gratefully acknowledge the financial support by the Ministry of Research and Technology Republic-Indonesia Program Penelitian Kerjasama antar Perguruan Tinggi (PKPT). The support activity by Yayasan Pengembangan IPTEK (YPIPT) Ichsan Gorontalo and Dept. of Electrical Engineering Universitas Hasanuddin-Gowa.

References

- [1] IEEE Std 519-2014 (Revision of IEEE Std 519-1992), "Recommended Practice and Requirements for Harmonic Control in Electric Power Systems," *The Institute of Electrical and Electronics Engineers*. 2014.
- [2] D. Kolokotsa, N. Kampelis, A. Mavrigiannaki, M. Gentilozzi, F. Paredes, F. Montagnino, and L. Venezia, "On the integration of the energy storage in smart grids: Technologies and applications," *Energy Storage*,

vol. 1, no. 1, p. 25 pages, 2019.

- [3] R. Pinto, S. Mariano, M R. Calado, and J F. De Souza, "Impact of Rural Grid-Connected Photovoltaic Generation Systems on Power Quality," *Energies, MDPI*, vol. 9, no. 9, pp. 1–15, Sep. 2016.
- [4] F. Ayadi, I. Colak, I. Garip, and H. I. Bulbul, "Impacts of renewable energy resources in smart grid," in *8th IEEE International Conference on Smart Grid, icSmartGrid2020, Paris-France*, pp. 183–188, Jun. 2020.
- [5] M. Patsalides, D. Evagorou, G. Makrides, Z. Achillides, G E. Georghiou, A. Stavrou, V. Efthymiou, B. Zinsser, W. Schmitt, and J H. Werner, "The effect of solar irradiance on the power quality behaviour of grid connected photovoltaic systems," *Renewable Energy and Power Quality Journal*, vol. 1, no. 05, pp. 323–330, Mar. 2007.
- [6] A. Amirullah, O. Penangsang, and A. Soeprijanto, "Power Quality Analysis of Integration Photovoltaic Generator to Three Phase Grid under Variable Solar Irradiance Level," *TELKOMNIKA (Telecommunication Computing Electronics and Control)*, vol. 14, no. 1, pp. 29–38, 2016.
- [7] A. Elkholy, F. H. Fahmy, A. A. Abou El-Ela, A. E.-S. A. Nafeh, and S. R. Spea, "Experimental evaluation of 8kW grid-connected photovoltaic system in Egypt," *Journal of Electrical Systems and Information Technology*, vol. 3, no. 2, pp. 217–229, 2016.
- [8] S. V. S. Kumary, V. A. A. M. T. Oo, G. M. Shafiullah, and A. Stojcevski, "Modelling and power quality analysis of a grid-connected solar PV system," in *Australasian Universities Power Engineering Conference, AUPEC, Perth-Australia*, pp. 1–6, Sep. 2014.
- [9] D. Gallo, R. Langella, A. Testa, J. C. Hernández, I. Papič, B. Blažič, and J. Meyer, "Case studies on large PV plants: Harmonic distortion, unbalance and their effects," in *IEEE Power and Energy Society General Meeting, Vancouver, BC-Canada*, pp. 1–5, 2013.
- [10] S. O. Amrouche, S. Bouchakour, A H. Arab, K. Abdeladim, F. Cherfa, and K. Kerkouche, "Reactive power issues in grid connected photovoltaic systems," in *International Conference on Nuclear and Renewable Energy Resources (NURER)*, pp. 1–6, 2014.
- [11] R. Kabiri, D. G. Holmes, and B. P. McGrath, "The influence of PV inverter reactive power injection on grid voltage regulation," in *IEEE 5th International Symposium on Power Electronics for Distributed Generation Systems (PEDG), Galway-Ireland*, pp. 1–8, Jun. 2014.

- [12] J. A. Sa'Ed, N. Ismail, S. Favuzza, M. G. Ippolito, and F. Massaro, "Effect of voltage deviations on power distribution losses in presence of DG technology," in *2015 International Conference on Renewable Energy Research and Applications, ICRERA*, pp. 766–771, 2015.
- [13] H. Li, C. Wen, K. H. Chao, and L. L. Li, "Research on inverter integrated reactive power control strategy in the grid-connected PV systems," *Energies, MDPI*, vol. 10, no. 7, pp. 1–22, 2017.
- [14] S. Vlahinić, D. Franković, V. Komen, and A. Antonić, "Reactive power compensation with PV inverters for system loss reduction," *Energies, MDPI*, vol. 12, no. 21, pp. 1–17, 2019.
- [15] IEEE Std 1547-2018, "Standard for Interconnection and Interoperability of Distributed Energy Resources with Associated Electric Power Systems Interfaces," *The Institute of Electrical and Electronics Engineers*, pp. 1–138, 2018.
- [16] K. Rahimi, A. Tbaileh, R. Broadwater, J. Woyak, and M. Dilek, "Voltage Regulation Performance of Smart Inverters: Power Factor Versus Volt-Var Control," in *North American Power Symposium (NAPS), Morgantown*, pp. 1–6, Sep. 2017.
- [17] F. Katiraei and M. R. Iravani, "Power management strategies for a microgrid with multiple distributed generation units," *IEEE Transactions on Power Systems*, vol. 21, no. 4, pp. 1821–1831, 2006.
- [18] W. Mack Grady and R. J. Gilleskie, "Harmonics and how they relate to power factor," in *EPRI Power Quality Issues & Opportunities Conference (PQA'93), San Diego, CA*, pp. 1–8, Nov. 1993.
- [19] A. Kalair, N. Abas, A. R. Kalair, Z. Saleem, and N. Khan, "Review of harmonic analysis, modeling and mitigation techniques," *Renewable and Sustainable Energy Reviews*, vol. 78, pp. 1152–1187, 2017.
- [20] M. Khatri and A. Kumar, "Experimental investigation of harmonics in a grid-tied solar photovoltaic system," *International Journal of Renewable Energy Research (IJRER)*, vol. 7, no. 2, pp. 901–907, Jun. 2017.
- [21] J. Vaquero, N. Vázquez, I. Soriano, and J. Vázquez, "Grid-connected photovoltaic system with active power filtering functionality," *International Journal of Photoenergy*, vol. 2018, no. Article ID 2140797, p. 9 Pages, 2018.
- [22] Q. T. Tran, A. V. Truong, and P. M. Le, "Reduction of harmonics in grid-connected inverters using variable switching frequency," *International Journal of Electrical Power and Energy Systems*, vol. 82, pp. 242–251, 2016.
- [23] C. Buccella, M. G. Cimatoroni, C. Cecati, L. A. Disim, and L. Aquila, "Low-frequency harmonic elimination technique in three phase cascaded H-bridges multilevel inverters for renewable energy applications," *International Journal of Smart Grid - ijSmartGrid*, vol. 3, no. 1, p. 9 Pages, 2019.
- [24] M. Karaca, A. Mamizadeh, N. Genc, and A. Sular, "Analysis of passive filters for PV inverters under variable irradiances," in *8th International Conference on Renewable Energy Research and Applications, ICRERA*, pp. 680–685, 2019.
- [25] M. Ayub, C. K. Gan, and A. F. A. Kadir, "The impact of grid-connected PV systems on harmonic distortion," in *IEEE Innovative Smart Grid Technologies - Asia (ISGT ASIA), Kuala Lumpur-Malaysia*, pp. 669–674, May 2014.
- [26] X. Xu, A. J. Collin, S. Z. Djokic, R. Langella, A. Testa, J. Meyer, and F. Möller, "Harmonic emission of PV inverters under different voltage supply conditions and operating powers," in *International Conference on Harmonics and Quality of Power (ICHQP), Belo Horizonte-Brazil*, pp. 373–378, Oct. 2016.
- [27] C. D. Crites, R. K. Varma, V. Sharma, and B. Milroy, "Characterization of harmonics in a utility feeder with PV distributed generation," in *IEEE Electrical Power and Energy Conference (EPEC), London*, pp. 40–45, Oct. 2012.
- [28] R. K. Varma, S. A. Rahman, T. Vanderheide, and M. D. N. Dang, "Harmonic impact of a 20-MW PV solar farm on a utility distribution network," *IEEE Power and Energy Technology Systems Journal*, vol. 3, no. 3, pp. 89–98, 2016.
- [29] L. Hassaine, E. Olias, J. Quintero, and M. Haddadi, "Digital power factor control and reactive power regulation for grid-connected photovoltaic inverter," *Renewable Energy*, vol. 34, no. 1, pp. 315–321, 2009.
- [30] S. Gonzalez, J. Neely, and M. Ropp, "Effect of non-unity power factor operation in photovoltaic inverters employing grid support functions," in *IEEE 40th Photovoltaic Specialist Conference (PVSC), Denver, CO, USA*, pp. 1498–1503, Jun. 2014.
- [31] Renukadevi V. and B. Jayanand, "Harmonic and reactive power compensation of grid connected photovoltaic system," in *Procedia Technology*, pp. 438–442, Jan. 2015.
- [32] N. N. Faizura Norhasmi, S. K. Raveendran, and V. K. Ramachandramurthy, "Power factor control of solar photovoltaic inverter as a solution to overvoltage," in *IEEE Asia-Pacific Power and Energy Engineering Conference (APPEEC), Kinabalu-Malaysia*, pp. 751–756, 2018.

- [33] W. Yi-bo, W. Chun-sheng, L. Hua, and X. Hong-hua, "Steady-state model and power flow analysis of grid-connected photovoltaic power system," in *IEEE International Conference on Industrial Technology, Chengdu-China*, pp. 1–6, Apr. 2018.
- [34] G. A. Rampinelli, F. P. Gasparin, A. J. Bühler, A. Krenzinger, and F. Chenlo Romero, "Assessment and mathematical modeling of energy quality parameters of grid connected photovoltaic inverters," *Renewable and Sustainable Energy Reviews*, vol. 52, pp. 133–141, 2015.
- [35] L. G. M. Oliveira, W. C. Boaventura, G. Amaral, J. V. G. C. Mello, V. F. Mendes, W. N. Macedo, P. F. Torres, A. S. Piterman, T.J.R. Corrade, and B. M. Lopes, "Assessment of harmonic distortion in small grid-connected photovoltaic systems," in *Proceedings of International Conference on Harmonics and Quality of Power (ICHQP), Belo Horizonte-Brazil*, pp. 810–815, Oct. 2016.
- [36] A. Elkholy, "Harmonics assessment and mathematical modeling of power quality parameters for low voltage grid connected photovoltaic systems," *Solar Energy*, vol. 183, pp. 315–326, May 01, 2019.